Updates on the rocking phenomenon

E.A.H. Vollebregt
VORtech CMCC, Delft, The Netherlands

ABSTRACT: Common models for wheel/rail contact typically start from a prescribed creepage or imposed contact force. This excludes the dynamical interaction between the two where each one responds to the other. This paper introduces a different approach where friction is related to the local deformation in and around the contact patch. This leads to forward and angular velocities that are oscillating with opposite phase, leading to the so-called rocking phenomenon. It is shown how the oscillation frequency depends on materials, geometry and normal load, and an experiment is proposed for validating this theory.

1 INTRODUCTION

The creep phenomenon was first described by Reynolds in 1876. It was used by Carter and Fromm for the analysis of the contact force in 2D steady rolling scenarios. That is, they considered situations in which the geometry, total force and creepage are held constant, such that time-invariant frictional stresses can be observed in a suitably defined coordinate system. Rolling contact theory was extended further by Johnson, who provided approximate solutions for 3D rolling with creep and spin, and Kalker, presenting full solutions for small creepages (linear theory) and for general concentrated contact (variational theory) (Kalker 1990).

Only few contributions deal with rolling contact under time-varying circumstances, such as changing normal load or varying creepage, which lead to time-varying tractions. The main result is due to Kalker, who found that transient efects die out quickly, within a traversed distance of a few contact widths (Kalker 1971; Kalker 1990). Similar conclusions were reached by Groß-Thebing and Knothe based on the analysis of harmonic variations (Groß-Thebing 1989; Knothe & Groß-Thebing 2008). However, those contributions start from an assumed contact force (Kalker) or reference state (Groß-Thebing). Including the interaction between creepage and force, we found that instationary effects may be relevant in a much wider range of circumstances (Vollebregt 2015).

This paper considers transient rolling scenarios, elaborating on the findings presented in the 2015 paper (Vollebregt 2015). It is shown how the contact force enters the dynamical equations. By changing the *a priori* assumptions, a new rocking phenomenon is found. It is then shown how the oscillation frequency depends on materials, geometry and normal load, and an experiment is proposed for validating the predictions.

2 DYNAMICS OF ROLLING MOTION

An idealized model is presented for the initiation of rolling of a sphere on a tilted plane. Three different choices are analyzed for modeling of the friction force: firstly assuming pure rolling without creepage, secondly assuming a constant creepage of 1%, and thirdly using a model that accounts for local elasticity in and around the contact point.

2.1 *Pure rolling,* $v = \omega r$

A coordinate system is used with x-direction tangential to the plane surface and z the outward normal direction (Fig. 1). Motion in normal direction is ignored. The degrees of freedom are

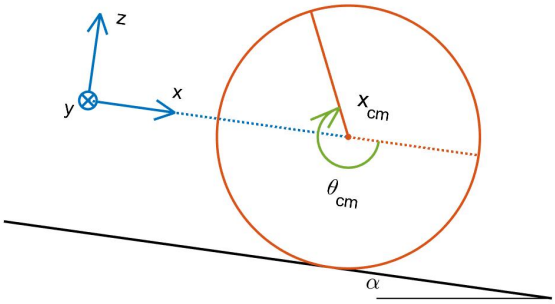

Figure 1. Idealized model of a sphere on an inclined plane: coordinate system & degrees of freedom.

$x = x_{cm}(t)$ for the position of the center of mass of the sphere and $\theta = \theta_{cm}(t)$ for the pitch angle, see Figure 1. The equations of motion for translational velocity v and angular velocity ω are

$$m\dot{v} = F_g + F_x, \tag{1}$$

$$I\dot{\omega} = -rF_x. \tag{2}$$

Here $F_g = mg\sin\alpha$ is the accelerating component of gravity along the plane, with α the tilt angle, and F_x is the friction force on the sphere in positive x-direction. The radius of the sphere is r and its moment of inertia is I.

The two equations have three unknowns, $\dot{v}, \dot{\omega}$ and F_x, therefore another equation is required. In many applications, it suffices to assume either full sliding or pure rolling, see for instance (Hibbeler 2012). The latter assumption is that $v = \omega r$, which gives $\dot{v} = \dot{\omega} r$. Inserting equations 1 and 2 gives

$$\frac{F_g + F_x}{m} = \frac{-rF_x}{I} \cdot r \quad \rightarrow \quad F_x = -\beta_0 F_g, \quad \text{with} \quad \beta_0 = \frac{I}{I + mr^2}. \tag{3}$$

This allows to eliminate F_x and to consider eqs. 1 and 2 separately. Starting from rest, with $x(0) = v(0) = \theta(0) = \omega(0) = 0$, this gives the solution

$$x(t) = \frac{(1-\beta_0)F_g}{m} \cdot \frac{t^2}{2}, \quad v(t) = \frac{(1-\beta_0)F_g}{m} \cdot t, \tag{4}$$

$$\theta(t) = \frac{r\beta_0 F_g}{I} \cdot \frac{t^2}{2}, \quad \omega(t) = \frac{r\beta_0 F_g}{I} \cdot t. \tag{5}$$

For a solid sphere the moment of inertia is $I = \frac{2}{5}mr^2$ such that $\beta_0 = \frac{2}{7}$ and $(1 - \beta_0) = \frac{5}{7}$.

2.2 *Constant creepage,* $v = 1.01\,\omega r$

Instead of pure rolling it could also be assumed that $v = 1.01\,\omega r$, amounting to a creepage of $\xi = (v - \omega r)/v = 1\%$. The analogue of equation 3 is

$$\frac{F_g + F_x}{m} = (1+\xi)\frac{-rF_x}{I} \cdot r \quad \rightarrow \quad F_x = -\beta_\xi F_g, \quad \text{with} \quad \beta_\xi = \frac{I}{I + (1+\xi)mr^2}. \tag{6}$$

This reduces the friction force slightly (at $\xi = 1\%$, $\beta_\xi = 0.2837$ instead of $\frac{2}{7} \approx 0.2857$), increasing v and reducing ω with respect to equations 4–5. Note however that the forces are constant in time such that uniform acceleration pertains.

Instead of imposing 1% creepage, we'd like to prescribe ξ such that the resulting F_x is on the creep force curve, $F_x = F_{crp}(\xi)$. This may be achieved in a few steps: computing F_x according to equation 3, looking up the corresponding creep value in $F_{crp}(\xi)$, computing F_x anew with eq. 6, and repeating until a balanced solution is found. Note that the creepage is imposed here as a constraint that's used to eliminate the contact force. A different strategy is used in vehicle dynamic simulation. There the contact force is kept in the equations, upon which the dynamics are used to find this equilibrium state.

2.3 *Accounting for local deformation*

The third choice for the friction force is to assume that it's proportional to the amount of elastic deformation in and around the contact zone. This is modelled here by assuming $F_x = K_x(\theta r - x)$. Here $\theta r - x$ describes the "lag" of translation with respect to rotation. A negative value means that the center of mass of the sphere has shifted somewhat down the plane, stretching the surface to the left, with friction F_x pointing to the left also. The factor K_x is a constant of proportionality, describing the stiffness of the surface.

This new choice for the contact force makes the equations of motion fully coupled between all four state variables:

$$\mathbf{M}\frac{\mathrm{d}\mathbf{y}}{\mathrm{d}t} = \mathbf{A}\mathbf{y} + \mathbf{f}, \quad \text{with } \mathbf{y} = \mathbf{y}(t) = \begin{bmatrix} x(t) \\ v(t) \\ \theta(t) \\ \omega(t) \end{bmatrix}, \quad \mathbf{M} = \begin{bmatrix} 1 & 0 & 0 & 0 \\ 0 & m & 0 & 0 \\ 0 & 0 & 1 & 0 \\ 0 & 0 & 0 & I \end{bmatrix}, \tag{7}$$

$$\mathbf{A} = \begin{bmatrix} 0 & 1 & 0 & 0 \\ -K_x & 0 & rK_x & 0 \\ 0 & 0 & 0 & 1 \\ rK_x & 0 & -r^2K_x & 0 \end{bmatrix}, \quad \text{and } \mathbf{f} = \begin{bmatrix} 0 \\ F_g \\ 0 \\ 0 \end{bmatrix}, \quad \text{and with } \mathbf{y}(0) = \mathbf{0}.$$

This is a linear system of ordinary differential equations of first order. The solution is constructed using a particular solution and the homogeneous solution. A particular solution fulfills the differential equation with right-hand side but may ignore the initial condition. A possible choice is the following:

$$\mathbf{y}_p = \begin{bmatrix} \frac{(1-\beta_0)F_g}{m}\frac{t^2}{2} + \frac{\beta_0 F_g}{K_x} \\ \frac{(1-\beta_0)F_g}{m}t \\ \frac{r\beta_0 F_g}{I}\frac{t^2}{2} \\ \frac{r\beta_0 F_g}{I}t \end{bmatrix}. \tag{8}$$

This looks like the pure rolling solution of equations 4–5, except that there's a constant negative lag $\theta r - x = -\beta_0 F_g / K_x$. This creates the friction force required to increase angular velocity.

The homogeneous solution is defined by the differential equation 7 with $\mathbf{f}$ set to $\mathbf{0}$. It is found by assuming $\mathbf{y} = \mathbf{c}e^{\lambda t}$. Inserting this in eq. 7 results in an eigenvalue problem

$$\mathbf{M}\lambda\mathbf{c}e^{\lambda t} = \mathbf{A}\mathbf{c}e^{\lambda t} \quad \rightarrow \quad \mathbf{M}^{-1}\mathbf{A}\mathbf{c} = \lambda\mathbf{c}. \tag{9}$$

The eigenfrequencies of the system are thus obtained by solving $det(\mathbf{M}^{-1}\mathbf{A} - \lambda\mathbf{I}) = 0$, which can be done analytically using the characteristic polynomial:

$$\lambda^2 \cdot \left(\lambda^2 + \frac{K_x r^2}{I} + \frac{K_x}{m}\right) = 0. \tag{10}$$

This has two roots $\lambda_1 = \lambda_2 = 0$, and two roots $\lambda_3, \lambda_4 = \pm i\sqrt{K_x(r^2/I + 1/m)}$. The eigensolutions are determined correspondingly, with coefficients c_1–c_4 that may be selected freely in order to fit the initial condition. After careful rewriting, the complete solution to the system of equation 7 is obtained as

$$\mathbf{y}(t) = \begin{bmatrix} \frac{(1-\beta_0)F_g}{m}\frac{t^2}{2} \\ \frac{(1-\beta_0)F_g}{m}t \\ \frac{r\beta_0 F_g}{I}\frac{t^2}{2} \\ \frac{r\beta_0 F_g}{I}t \end{bmatrix} + \frac{m\beta_0^2 F_g}{K_x} \cdot \begin{bmatrix} \frac{1}{m}\left(1 - \cos(\bar{\lambda}t)\right) \\ \frac{\bar{\lambda}}{m}\sin(\bar{\lambda}t) \\ -\frac{r}{I}\left(1 - \cos(\bar{\lambda}t)\right) \\ -\frac{r\bar{\lambda}}{I}\sin(\bar{\lambda}t) \end{bmatrix}, \quad \text{with } \bar{\lambda} = |\lambda_3|, \tag{11}$$

$$F_x(t) = -\beta_0 F_g \left(1 - \cos(\bar{\lambda}t)\right). \tag{12}$$

This shows an undamped oscillation superimposed on the uniform acceleration solution for pure rolling. The friction force oscillates between 0 and 2 times the equilibrium value needed for pure rolling. The position $x(t)$ is ahead of the pure rolling solution by a distance $\beta_0^2 F_g / K_x$ on average, which is also the oscillation amplitude.

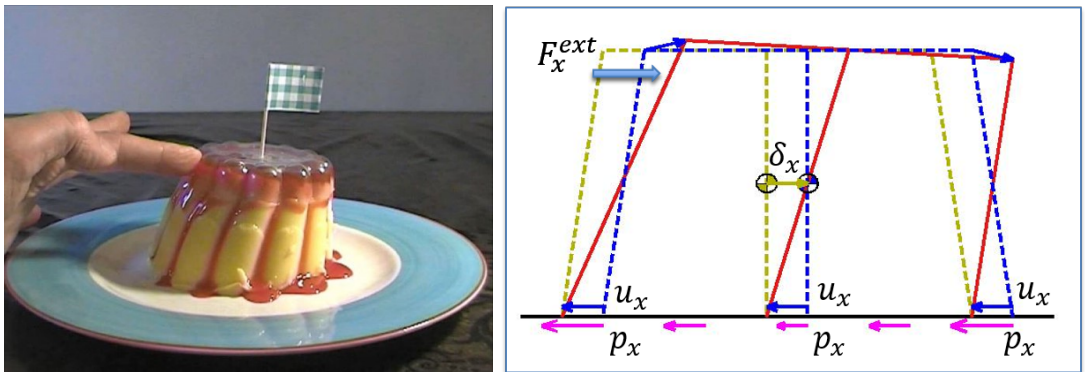

Figure 2. Physical interpretation of equation 16: below the Coulomb maximum, the body will deform precisely as much as needed –shifting the center of mass– to prevent overall sliding.

3 THE ROCKING PHENOMENON

This in-plane oscillation is termed the rocking phenomenon (Vollebregt 2015). It occurs by rigid body translation and rotation in combination with a harmonically oscillating contact force.

The main assumption that leads to rocking is that the contact force responds to the lag, $F_x = K_x(\theta r - x)$. This formula was found to mimic the behaviour of a complete model comprising the dynamical equations 1–2 and the full CONTACT model for the calculation of the contact force (Vollebregt 2017b). Without micro-slip, the lag $\theta r - x$ corresponds to the displacement u_x^{avg} of the contact patch relative to the wheel center of mass. This is illustrated schematically in Figure 2 (Vollebregt, in prep.).

This analysis is supported by simple manipulations on the basis of the half-space approach. There, the elastic displacement u_x in x-direction is computed using an integral of surface tractions p_x:

$$u_x(x,y,t) = \iint_C A_{xx}(x,y,x',y')\, p_x(x',y',t)\, dx'\, dy'. \tag{13}$$

The kernel A_{xx} comes from the well-known Boussinesq-Cerruti solution (Kalker 1990). There are contributions of p_y and p_n as well that are of secondary importance for the current discussion.

With A_c the contact area, the average displacement over the contact patch may be written as

$$u_x^{avg}(t) = \frac{1}{A_c} \iint_C u_x(x,y,t)\, dx\, dy \tag{14}$$

Inserting equation 13 and exchanging the integrals gives

$$u_x^{avg}(t) = \iint_C \left(\frac{1}{A_c} \iint_C A_{xx}(x,y,x',y') dx\, dy \right) p_x(x',y',t)\, dx'\, dy' \tag{15}$$

The term in parenthesis concerns a flexibility $L_{xx}(x',y')$ that's only moderately dependent on the position (x',y'). Approximating this by an average value yields

$$u_x^{avg}(t) \approx L_{xx}^{avg} F_x(t) \quad \leftrightarrow \quad F_x(t) \approx K_x u_x^{avg}(t). \tag{16}$$

In the CONTACT program, the stiffness K_x can thus be computed using the column sums of the matrix of influence coefficients. For the user, the stiffness is obtained using the Cattaneo shift problem, $K_x = F_x/\delta_x$, for a shift δ_x that yields a vanishingly small slip area.

4 EXPERIMENTAL VALIDATION

It is generally difficult to measure contact forces precisely, and this is particularly true for demonstrating the rocking phenomenon. A detailed measuring principle should be used that does not disturb the rocking itself.

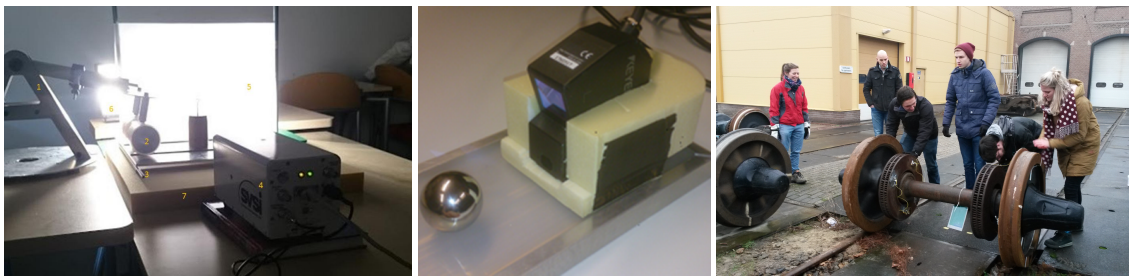

Figure 3. Experimental set-ups used by students of Saxion Hogeschool in 2015–2016, using a cylinder and high-speed camera (left), sphere with laser triangulation sensor (middle) and wheel-set with accelerometers (right, supported by NedTrain).

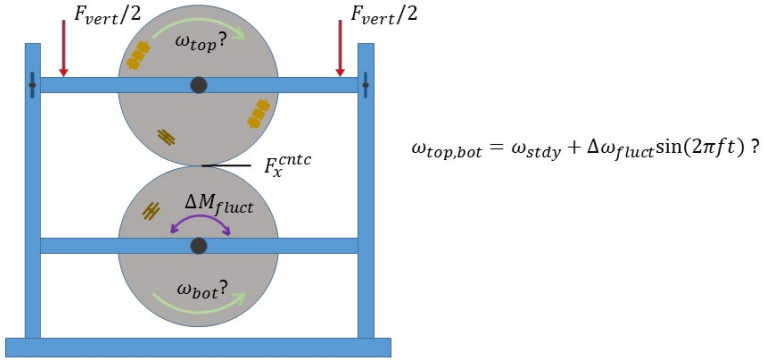

Figure 4. Proposed experimental set-up: the rollers are rotating at some speed $\pm\omega_{stdy}$, then a torque fluctuation is added with amplitude ΔM_{fluct}. A considerably bigger speed fluctuation $\Delta\omega_{fluct}$ is predicted at the rocking frequency.

Table 1. Proposed parameter values for the experimental set-up of Figure 4.

Soft materials	E_{rubber}	15	N/mm^2	ν_{rubber}	0.5	–
Dimensions	r	100	mm	h	60	mm
	m	2	kg	I	10^4	kg mm^2
Point contact	r_{crown}	100	mm	F_{vert}	−15–100	N
Free rolling	ω_{stdy}	5–20	rpm	M_{stdy}	≈ 0	N mm
Imposed torque	f_{fluct}	20–100	Hz	ΔM_{fluct}	10–200	N mm
→ Rocking at	f_{rock}	42–72	Hz	K_x^{cntc}	36–103	N/mm

4.1 *Preliminary experimentation*

Preliminary experiments were done in 2015–2016 by 27 students of Saxion Hogeschool in Enschede, The Netherlands. Different approaches were explored by teams of 4–5 students: using a steel cylinder with rubber coating, a steel sphere or an actual wheel-set, and using a high-speed camera, laser triangulation or accelerometers (Fig. 3). This has provided useful insights in the problem, but no usable measurement data have been obtained thusfar.

From the experiments we conclude that the overall distance traversed provides a main source of difficulties for the optical measuring techniques (Fig. 3, left & middle). When using accelerometers on an actual wheel-set, the difficulty is to start rolling with rocking included. The wheel-set is too heavy to initiate this by hand (Fig. 3, right), whereas a test-rig often has vibrations in the structure that may interact with the rocking phenomenon.

4.2 *Proposed experiment*

Figure 4 proposes a new approach for experimentation. Instead of using a step response, starting from rest, this seeks to demonstrate rocking using resonance. The rollers are first brought into a steady rolling motion at some speed ω_{stdy}. Then the motor torque is set to oscillate at a predefined frequency. The question is how the two rollers respond.

If reality is like pure rolling, the rollers will rotate with $\omega_{top} = -\omega_{bot}$, upon which the amplitude of the speed fluctuation will be found as

$$\Delta\omega_{fluct} = \frac{\Delta M_{fluct}}{4\pi I f_{fluct}}. \tag{17}$$

For the parameters of Table 1 this is in the range of 0.05–$5\,\mathrm{rpm}$.

On the other hand, if there's a tangential contact stiffness K_x^{cntc}, then there will be resonance at the rocking frequency. This means that $\Delta\omega_{fluct}$ will grow over time until it's restricted by damping and non-linear effects, resulting in a much larger speed fluctuation.

For the situation of two rollers that are confined such that no translation occurs, the rocking frequency is found as

$$f_{rock} = \frac{1}{2\pi}\sqrt{10^3 K_x^{cntc}\frac{2r^2}{I}}. \tag{18}$$

The factor 10^3 stems from using mm as the unit of length. Using Hertz theory and the Cattaneo shift problem, the stiffness is found as

$$K_x^{cntc} = \alpha(k)\frac{2\sqrt{ab}E}{(2-\nu)(1+\nu)}. \tag{19}$$

Here $\alpha(k)$ is a shape factor for ellipticity $k = a/b$: $\alpha(k) \approx 1$ for $1/3 < k < 3$, and $\alpha(k) \approx 2$ for very wide or elongated contact ellipses. For circular contacts and Poisson ratio $\nu = 0.5$ this is approximated further as

$$a = \left(\frac{3F_n R^*}{4E^*}\right)^{1/3}, \quad E^* = \frac{E}{2(1-\nu^2)}, \quad R^* = \frac{r}{2}, \tag{20}$$

$$K_x^{cntc} = \frac{2E}{(2-\nu)(1+\nu)} \cdot \left(\frac{3F_n r(1-\nu^2)}{4E}\right)^{1/3} \approx \left(0.4 r F_n E^2\right)^{1/3}. \tag{21}$$

(A slight error was corrected in November 2020, thanks to Ahmad Radmehr.) Predicted values for f_{rock} and K_x^{cntc} are listed in Table 1 for the suggested values of the other parameters.

5 CONCLUSIONS

Simulations with the CONTACT model integrated in dynamical models for rolling motion exhibit an in-plane oscillatory motion that's called the rocking phenomenon. This behaviour is explained by noting a rough proportionality between the contact force and the elastic displacement in/around the contact patch relative to the center of mass of the roller. The same behaviour is obtained using a simplified model using a linear spring element. A new set-up is proposed to test these predictions experimentally.

REFERENCES

Groß-Thebing, A. (1989). Frequency-dependent creep coefficients for three-dimensional rolling contact problems. *Vehicle System Dynamics* 18(6), 359–374.

Hibbeler, R. (2012). *Engineering Mechanics - Statics and Dynamics, 13th Edition*. Upper Saddle River, New Jersey: Pearson Prentice Hall.

Kalker, J. (1971). A minimum principle for the law of dry friction. Part 2: Application to nonsteady rolling elastic cylinders. *Journal of Applied Mechanics* 38, 881–887.

Kalker, J. (1990). *Three-Dimensional Elastic Bodies in Rolling Contact*, Volume 2 of *Solid Mechanics and its Applications*. Dordrecht, Netherlands: Kluwer Academic Publishers.

Knothe, K. & A. Groß-Thebing (2008). Short wavelength rail corrugation and non-steady-state contact mechanics. *Vehicle System Dynamics* 46(1-2), 49–66.

Vollebregt, E. (2015). New insights in non-steady rolling contact. In M. Rosenberger (Ed.), *Proceedings of the 24th International Symposium on Dynamics of Vehicles on Roads and Tracks*, Graz, Austria. IAVSD.

Vollebregt, E. (2017a). Current understanding of the creep phenomenon. *In preparation*.

Vollebregt, E. (2017b). User guide for CONTACT, Rolling and sliding contact with friction. Technical Report TR09-03, version 17.1, VORtech. See `www.kalkersoftware.org`.